Survey of Low-Power Wireless Network Technologies for the Internet of Things

Niklavs Barkovskis, Kaspars Ozols, Atis Elsts
Institute of Electronics and Computer Science (EDI)
Riga, Latvia
niklavs.barkovskis@edi.lv, kaspars.ozols@edi.lv, atis.elsts@edi.lv

***Abstract*—A large number of different low-power wireless network technologies exist, including IEEE 802.15.4, Bluetooth Low Energy, multiple protocol standards of WiFi (IEEE 802.11), Near Field Communication (NFC), and LoRa. Given this number of competing technologies, the selection of the best one for a new project is not trivial. This paper aims to help Internet of Things (IoT) practitioners in this task. To this end, we illuminate the underlying technical differences between these state-of-the-art wireless solutions through their assessment and brief analysis. We quantify and compare their latency, throughput and overhead, as well as overview their main characteristics such as frequency bands, bandwidth, medium access methods, and packet sizes.**

I. Introduction

The number of IoT devices is growing with astounding speed. The total number of connected devices in 2016 is estimated to be 6 billion, while in 2020 this number is estimated to increase to 20 billion [1]: in other words, the yearly growth rate is 20–30 %. IoT has a great potential to impact many businesses, and has thousands of use cases in situation where wireless connectivity is required or beneficial. Low-power wireless networks are used in many application areas, including intelligent transportation systems [2], [3], healthcare and fitness [4], smart cities [5], smart homes [6], Industry 4.0 [7] and others.

When considering a new IoT project, the following question often arises: "Which wireless technology is the best for the project's requirements?" The choice of a wireless technology impacts the functionality and other aspects of the final result, including energy efficiency, throughput, latency, reliability, security and range. This paper aims to help IoT practitioners to answer this question.

The choice of wireless solution highly depends on the device, environment and application requirements. The numerical parameters of the wireless radio typically can be found in its datasheet, provided by its manufacturer. For example, the datasheet of the Nordic nRF52840 [9] System-on-Chip includes the nominal data rates and power consumption numbers of this device in different radio modes: Bluetooth Low Energy (BLE), IEEE 802.15.4, and a proprietary mode. However, the nRF52840 datasheet does not include a derived information such as the minimum latency achievable at a specific packet size, and does not give clear understanding of the different radio modes and how they affect throughput, latency, packet overhead, communication reliability, interference and range. The same limitations apply to other typical datasheets. All these aspects are necessary to understand the suitability and the limitations of a given device and technology.

In view of this problem, this paper makes the following contributions:

- Analysis of state-of-the-art wireless technologies with focus on PHY and MAC layers.
- Analytic models for relations between the payload size, configuration parameters, and packet duration, for each of the technologies. We utilize the models to visually show the dependence of the throughput and latency on the payload size.
- Comparison between these state-of-the-art technologies, including quantitative comparison in terms of packet overhead, latency, and throughput.

Our paper surveys wireless network technologies in an application-agnostic way, without assuming specific channel loss models or network topologies.

The structure of this paper is as follows. Section II surveys and analyses state-of-the-art wireless technologies. Section III provides a higher-level discussion and comparison between the technologies, as well as sketches the overall trends in this space. Section IV describes related work, and Section V concludes this paper.

II. Low-Power Wireless Technologies

A. Overview

The electronics industry, especially consumer and manufacturing electronics, use the so-called Industrial, Scientific and Medical (ISM) radio bands. These ISM bands (Table I) are internationally recognized. Other wireless communication bands are region-specific, defined by national governments, and their uses include broadcasting, radio navigation, mobile communications, meteorological-satellite, space and earth research [10].

Technologies that use licensed spectrum bands (e.g., GSM, LTE) are standardized by ITU or ETSI standardization organizations. This is not the case for unlicensed bands. They are standardized by informal standardization organizations, such as The Institute of Electrical and Electronics Engineers (IEEE) [11].

The research leading to these results has been supported by the ECSEL Joint Undertaking under grant agreement No. 737453 (I-MECH) [8]. This Joint Undertaking receives support from the European Union Horizon 2020 research and innovation program and the ECSEL member states.

TABLE I
ISM RADIO BANDS

Frequency band	Bandwidth	Type[12]
6.765–6.795 MHz	300 KHz	Wireless charging
13.553–13.567 MHz	14 KHz	Near field
26.957–27.283 MHz	326 KHz	Long range
40.66–40.7 MHz	40 KHz	Long range
433.05–434.79 MHz (Region 1)	1.74 MHz	Long range
863–868 MHz (Region 1)	5 MHz	Mid-range
902–928 MHz (Region 2)	26 MHz	Mid-range
2.4–2.5 GHz	1000 MHz	Short range
5.725–5.875 GHz	150 MHz	Short range

Region 1 – Europe, Africa, Russia and Middle East; Region 2 – Americas, including Greenland [10]

Unlicensed does not mean unregulated: regulatory agencies place limitations on the operating frequencies, output power, spurious emissions, modulation methods, and transmit duty cycles among other things. The purpose of the standards operating in the unlicensed bands is to ensure effective interoperability between products from different vendors, recognizing the need for taking advantage of technology development for commercial use [11]. A drawback is that there is no registry of unofficial wireless standards. However, a number of low-power wireless technologies (Table II) can be unofficially identified as widely used at the time of writing. We focus on these technologies.

B. Assumptions and Metrics for the Technology Analysis

The characteristics found in Table II form a basis for the further analysis in this paper, which aims to allow the reader to objectively compare different wireless solutions.

To make the technology comparison fair, we use an application-agnostic setup and assume a perfect channel (a channel with no loss). Introducing specific losses in the channel either make this analysis application-specific, or impossible to include to in a single paper due do the number of different loss modes observable in different real-world setups.

We assume that the communication mode is point-to-point, that no encryption is used, and that a connection is already established if the technology is connection-oriented. These assumptions are maximally general, while at the same time reduce the scope sufficiently to make this analysis feasible within a single paper.

We look at the following metrics in more detail:

- *Latency* (T_{event}). This is defined as the time between the request to transmit a packet and the reception of an acknowledgment, and includes the time for transmission of the request and acknowledgment (ACK) frames, as well as inter-frame spacing, and other delays specified by a communication protocol standard.
- *Throughput.* This is defined as the number of payload bytes that can be sent in one second during an active connection, where number of packets sent per second is calculated as $1/T_{event}$.
- *Payload length.* This is defined as the range of payload bytes permitted to be included in a single packet by the wireless technology standard.

C. Near Field Communication (NFC)

The roots of NFC are in the Radio Frequency Identification (RFID) technology. RFID standards such as ISO 14443 operate at f_c=13.56 MHz frequency range. However, these standards are not further analyzed in this paper as they allow only one-way communication, and define only the physical layer.

The Near Field Communication (NFC) standard [20], on the other hand, standardizes three modes of operation: Peer-to-peer, Reader-Writer and Card emulation. The Reader-Writer mode enables host to read and write data stored into the tag. The Card emulation mode allows host to act as the tag. These modes allow only one-way communication.

The Peer-to-Peer Mode supports user level communication between two parties by utilizing Simple NDEF Exchange Protocol (SNEP), which resembles the top half of the OSI model's Data Link Layer. NFC Data Exchange Format (NDEF) messages are put into Logical Link Control Protocol (LLCP), which is encapsulated in Data Exchange Protocol (DEP) built on top of the physical layer (ISO 14443) – the whole radio layer stack is standardized as Interface and Protocol (NFCIP-1) standard or ISO/IEC 18092. Devices support three raw bitrates: $f_c/_{32}$, $f_c/_{64}$ and $f_c/_{128}$ corresponding to bit duration of $T_{bit} = 1/f_c$ or 2.35 μs, 4.72 μs and 9.4 μs respectively [20].

NDEF encapsulates one or more application-defined payloads in a standardized format for storing formatted data on NFC tags (used in the Reader/Writer mode), therefore preserving the interoperability of communication. This hierarchy is shown in Fig. 1.

Start	Length	Payload (2 – 255 bytes)							CRC
		DEP Flags	LLCP Flags	Sequence (optional)	Data (0 – 128 bytes)				
1 or 8 bytes f_{128} or f_{64}, f_{32}	1 byte	5 bytes	2 bytes	1 byte	Version	Code	Length	NDEF data	2 bytes
					1 byte	1 byte	4 bytes	Up to 122 bytes	

Fig. 1. NFC NDEF packet format

When a communication event happens, the receiver acknowledges the packet with a response. The response has a minimum delay of T_{Delay}=37.76 μs. The response packet contains L_{resp}=1 byte of ACK bits in payload field and the command bits of *DEP* field set to response code [21], where the request packet L_{packet} contains a variable number (N) of payload bytes:

$$T_{event} = 8 \cdot T_{bit} \cdot L_{resp} + 8 \cdot T_{bit} \cdot L_{packet}(N) + 2 \cdot T_{Delay}$$

$$L_{packet}(N) = L_S + L_H + N + L_{CRC}$$

In $f/_{32}$ and $f/_{64}$ modes, L_S=8, since preamble is 7 bytes longer compared with the $f/_{128}$ mode, to ensure better synchronization in shorter symbol periods. The length of headers is L_H=15 bytes, which includes 1 byte *Length*, 5 byte *DEP* and 2 byte *LLCP* field, 1 byte sequence field and 6 byte *NDEF* protocol header, terminated with L_{CRC}, which is 2 bytes long.

TABLE II
PHYSICAL LAYER CHARACTERISTICS OF WIRELESS TECHNOLOGIES

	Frequency band	Channels	Channel width	Modulation	Coding scheme
NFC [13]	13.56 MHz	1	14 KHz	10/100 % ASK	Miller coding
LoRa [14]	868 MHz (EU)	9/1 up/down (EU)	125/250 kHz (EU)	CSS	ALOHA
	915 MHz (US)	72/8 up/down (US)	125/250/500 kHz (US)		
IEEE 802.15.4 [15]	2.4 GHz	16	5 MHz	O-QPSK, CSS	DSSS
IEEE 802.15.4 [15]	868MHz (EU)	1	600 kHz	O-QPSK, BPSK, ASK	DSSS
	915 MHz (US)	10	2 MHz		
Bluetooth LE [16]	2.4–2.4835 GHz	40	2 MHz	GFSK	Adaptive FHSS
IEEE 802.11b [17]	2.4 GHz	11 (US)	22 MHz	DBPSK, DQPSK	CCK/PBCC/DSSS
		11 (US)			
IEEE 802.11g [18]	2.4 GHz	13 (EU),	22 MHz	BPSK – 64QAM	ERP-OFDM
		11 (US)	(2 MHz guard)		DSSS-OFDM
IEEE 802.11n [19]	2.4 GHz	13(EU), 11(US)	22 MHz	BPSK – 64QAM	HT-OFDM
	5 GHz	24 (EU&US)	2*20=40 MHz		

BPSK/QPSK/O-QPSK/GFSK/PSK/ASK – Binary/Quadrature/Offest-Quadrature/Guassian/Phase/Amplitude Phase Shift Keying; CSS – Chirp Spread Spectrum; DSSS – Direct-sequence spread spectrum; OFDM – Orthogonal frequency-division multiplexing; FH – Frequency hopping; CCK – Complementary Code Keying;

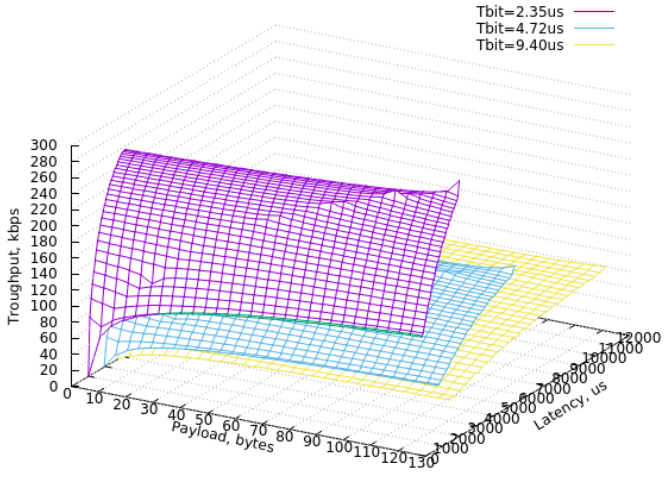

Fig. 2. NFC payload length vs. latency and throughput

Fig. 2 displays the throughput achievable in the $f/_{32}$, $f/_{64}$ and $f/_{128}$ modes and the respective latency. The results are 296 kbps / 3.29 ms, 149 kbps / 6.53 ms and 82 kbps / 11.8 ms for each of the modes, respectively, when sending the maximum payload of 122 bytes. The minimum delays, when sending 1 byte packets, are 1015 μs, 1963 μs and 2782 μs, respectively.

It is important to note that NFC operates in the near-field reactive region, which is bounded by the size of the wavelength λ. The near-field region ends at $\lambda/2\pi$ distance. For λ=22 m in case of 13.56 MHz frequency, $\lambda/2\pi$=3.52 m. Since the NFC specification aims for operating range of 4–10 cm, its antennas are typically shorter than $\lambda/4$ [20]; in contrast, for far field antennas, sizes of $\lambda/2$ and $\lambda/4$ are typical (e.g., the well-known half-wave dipole and quarter-wave monopole antennas).

D. LoRa and LoRaWAN

LoRa (Long Range) is a proprietary low-power wireless technology created and owned by Semtech. The signal in LoRa is modulated by a variant of Chirp Spread Spectrum (CSS) modulation [22], with integrated Forward Error Correction (FEC). CSS is used with the aim to provide a longer range. It has a great resistance against multi-path fading, when using pseudo-orthogonal spreading of chirps [23]. LoRa receivers have extremely high sensitivity compared with the rest of the surveyed technologies: on the order of -130 dBm.

LoRa uses a number of tunable parameters, including[22]:

- Spreading Factor (*SF*): is the ratio between the nominal symbol rate and chirp rate;
- Transmission Power (TP): the signal strength, up to 20 dBm;
- Carrier Frequency (CF): the center frequency of the signal;
- Bandwidth (BW): the width of the frequencies in the transmission band;
- Coding Rate (CR): the rate of the FEC code used in transmissions.

The LoRa technology itself refers only to the the PHY layer and can be used in conjunction with different MAC layers. However, the LoRa Alliance also defines the LoRaWAN standard [24], which is an associated set of specifications that defines an upper-layer network stack meant to be used on top of LoRa.

The LoRaWAN specification defines three different device types [22], [25]. Class A devices support uplink communication (from device to a gateway) at random, and a very limited form of downlink communication: namely, a device opens a short receive window after transmitting its own message. Class B devices allow more extensive bidirectional communication through scheduled slots for reception. Class C devices always keep their radio on for reception. Class A and B devices typically are battery powered, while class C devices – mains powered.

The LoRaWAN packet structure is shown in Fig.3. Every packet starts with a preamble [14], which determines the modulation scheme for the rest of the packet. The preamble starts with a sequence of at least 6 constant upchirps, followed by two symbols that encode a sync word (0x34 in the

Preamble	PHY Header (explicit mode)	PHY Header CRC (explicit mode)	PHY Payload (2 to 255 bytes)									CRC (uplink)
			MAC Header (1 byte)			MAC Payload					MIC	
			Mtype	RFU	Major	Frame Header				Fport	Frame Payload		
At least 10.25 symbols	2 bytes	2 bytes	3 bits	3 bits	2 bits	DevAddr	Fctrl	Fcnt	Fopts	1 byte	Up to 244 bytes	4 bytes	2 bytes
						4 bytes	1 byte	2 bytes	0-15 bytes				

Fig. 3. LoRaWAN packet format

European Union). The sync word is followed by two and a quarter downchirps (2.25 symbols), making the total length of preamble at least L_{PRE}=10.25 symbols. The symbol duration is T_s, and depends on *BW* and *SF* parameters. The rest of the packet is transmitted with bit duration T_b and encoded with a specific Code Rate (*CR*) to increase the reliability of the transmission. The FEC used in LoRa is based on Hamming codes. If LoRaWAN is configured to be in the Explicit mode, a packet contains 19 bytes of configuration information. In the Implicit mode, these 19 optional bytes are not present.

In the European Union, LoRa uses 125 kHz and 250 kHz bandwidth (*BW*). The LoRaWAN specification states that there should be at least eight available frequencies, but only the three first ones (all 125 kHz) are compulsory for a communication [24].

Further analysis assumes that a strict and scheduled request-response model is used, i.e., Class B, and that communication is configured in the implicit mode. LoRaWAN is not a real-time wireless technology, therefore a receive window is typically active 1 sec +/-20 μs after an uplink message. However, to acquire the maximum throughput, which is necessary for this comparison, it is assumed that the Inter-frame Space T_{IFS} equals to 5 ms, which is highly recommended to achieve acceptable PER (Packet Error Rate) [26].

Lastly, to address the precise relation between throughput and latency in LoRaWAN, it is important to note that the channels used in 868 MHz band are restricted to 1% duty cycle for transmissions [27]. On the average, a single device can occupy the medium for 10 ms in 1 sec, or 36 seconds in one hour. It is also noted that the minimum off time between two consecutive transmissions in same channel is 1.8 sec, and maximum duration of an individual transmission is 3.6 s. Therefore calculations assume that only one packet is sent per one second. As shown further with *SF*=12 and *CR*=4/5, not even a single full packet can be sent during the one second period.

LoRa packet length (Fig. 3) depends on the length of the preamble, headers (L_H), and on a variable-length payload (N_P). The PHY header length L_{PHY} depends on four byte fields. However, they are included only in explicit mode, therefore not relevant in this analysis. The MAC header L_{MH} size is one byte, frame header is L_{FH}=7 bytes long, with optional 15 byte options field that is used for commands to change throughput, transmit power, validate connection, and for other purposes. The *FPort* field, which is L_{PORT}=1 byte long, is used to distinguish between data or MAC commands used in payload. The *MIC* field is the digital signature of the message, and is L_{MIC}=4 bytes long. The CRC field, which is L_{CRC}=2 bytes long is used only in uplink messages, but not in downlink, which

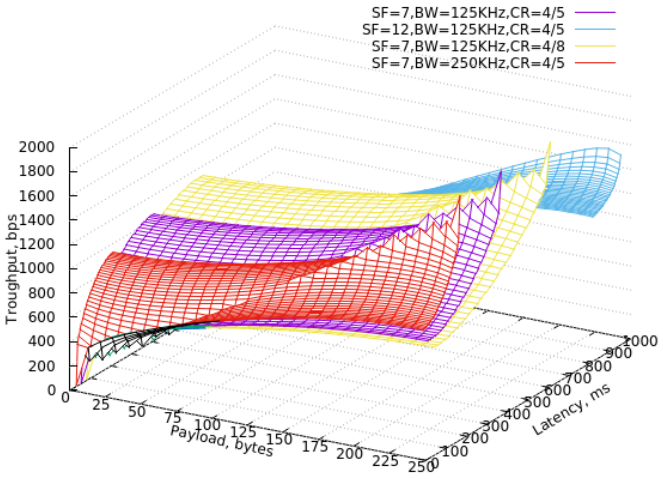

Fig. 4. LoRa payload length vs. latency and throughput

makes L_H=13 bytes long when assessing T_{ACK}, but 15 bytes long when assessing $T_{frame}(n)$.

$$T_b = \frac{2^{SF}}{SF \cdot BW \cdot CR};\ CR = \frac{4}{4+n};\ SF \in 7...12;\ n \in 1...4$$

$$T_{event} = T_{frame}(n) + T_{IFS} + T_{ACK} + T_{IFS}$$

$$T_{frame}(n) = T_c \cdot L_{PRE} + 8 \cdot T_b \cdot (L_H + N_P)$$

$$L_H = L_{PHY} + L_{MH} + L_{FH} + L_{PORT} + L_{MIC} + L_{CRC}$$

Fig. 4 shows four scenarios and demonstrates that increasing the spreading factor vastly increases communication latency. In most cases this is not important, since the duty cycle of a transmission is restricted by EU regulatory rules, and the same amount of data can be sent during one second (one uplink and one downlink message). The main trade-off here is the power consumption vs. receiver sensitivity, since more chirps increase power requirements for a transmission, but at the same time facilitate the decoding of the signal.

Since only one packet can be sent during the whole one second period, regardless of the selected *CR* and *SF* values, the maximum throughput is 243×8=1944 bps. When sending 1 byte packets, depending on scenario, the delay is 57 ms, 885 ms, 83 ms and 33.4 ms. Full 244 byte packets cannot be transmitted when *SF*=12, because bit period is about 18 times bigger (34 ms) than when *SF*=7 (1.8 ms). In this case, the maximum throughput is only 800 bps and latency the maximum (1000 ms). In other cases, the full packet latency is 412 ms, 651 ms and 211 ms.

E. IEEE 802.15.4

The IEEE 802.15.4 standard defines PHY and MAC layers and allows vendors and developers to build the link-to-application layer protocol stack. There are many upper-layer protocols for IEEE 802.15.4 networks, for example WirelessHART, OpenThread and ZigBee. The IEEE 802.15.4 MAC layer includes a large number of configuration parameters,

including flexible control over timing and network topologies. Multihop mesh is among the topologies that can be built on top of IEEE 802.15.4, in contrast to other, less flexible low-power wireless technologies that focus on point-to-point or star topologies. As in other protocols, the IEEE 802.15.4 MAC layer includes packet retransmissions. Upper layer protocols (e.g., ZigBee) take care of handling routing, connection establishment and other networking aspects.

An IEEE 802.15.4 MAC layer packet is shown in Fig. 5.

Preamble	Start of Frame	Frame Length	PHY Payload (0 – 127 bytes)				
			MAC Frame control	Sequence number	Addressing fields	MAC payload	Frame Checksum
4 bytes	1 byte	1 byte	2 bytes	1 byte	0-20 bytes	Up to 122 bytes	2 bytes

Fig. 5. IEEE 802.15.4 frame format

IEEE 802.15.4 defines various PHY configurations, but mainly ASK, BPSK or QPSK modulation is used in combination with DSSS coding, which helps to reduce overall signal interference. The DSSS technique works by modulating the message with a pseudo-random sequence of bits. The resulting signal has nearly the same bandwidth as that of the pseudo-random sequence. The larger the resulting bandwidth compared with the bandwidth of the message itself, the more robustly the message is protected against errors. In IEEE 802.15.4, the DSSS is implemented by mapping 4-bit symbols of data to the set of 32-bit code-words. Each code-word can be decoded even if it has multiple corrupted bits. In the 2.4 GHz frequency band, the duration of a 4-bit IEEE 802.15.4 symbol is T_s=16 μs and the duration of a single code-word bit is T_b=0.5 μ [15].

The initial versions of the standard [15] define two main communication modes: beacon enabled and non-beacon enabled. In IEEE 802.15.4-2015, additional modes are added, including the Time Slotted Channel Hopping MAC mode [28]. The beacon mode uses guaranteed time slots for scheduled data transmissions between gateway and nodes. The non-beacon mode is used for asynchronous data transmission, where a device listens the medium before transmitting (the "Listen Before Talk" technique). The CSMA/CA (Carrier-Sense Multiple Access/Collision Avoidance) algorithm [29] is used to decide when to backoff from sending, and when to send the packet. This non-beacon mode is used in the further analysis.

A backoff delay T_{BO} is introduced in the standard to reduce the probability of collisions among contending nodes. Its value is expressed as the number of 320 μs long backoff slots. The number of backoff slots used is a random number in the interval (0, $2^{BE}-1$), where *BE*, the backoff exponent, is set to the initial value of 3 [15]. Since our analysis focuses on point-to-point data transfers, there are no other contending nodes, therefore wee assume that backoff delay equals to the average of *BE* as T_{BO}=320$\times$(2^3-1)=1120 μs.

After completing its backoff, the node performs a clear channel assessment. If, after eight symbol periods (T_{CCA}=8$\times T_S$), the channel is assessed to be free, the data frame can be transmitted. If an acknowledgment has been requested,

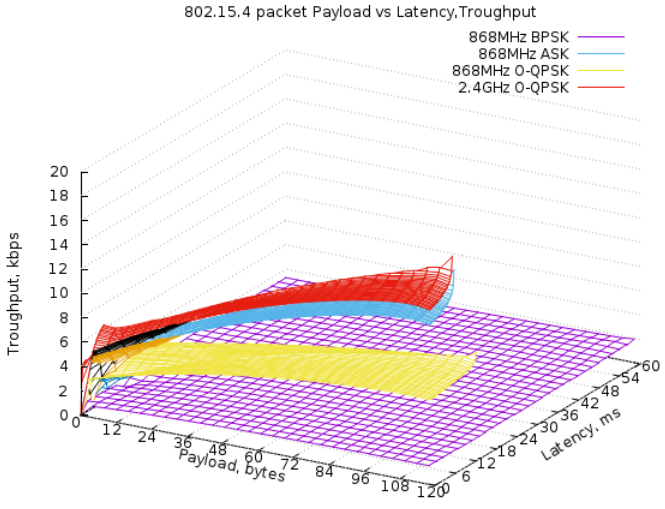

Fig. 6. 802.15.4 payload length vs. latency and throughput

after the packet is received, the receiver sets a timer that triggers at T_{TA}=192 μs (turnaround time) that allows the sender to switch to receiving mode, and the receiver to transmitting mode.

The equations below are a slight modification of the ones present in [30]. The difference is that our work includes variable payload size and involves T_{CCA} latency with ability to calculate characteristics for different bit rates. Further, we assume that short addressing mode is used, without the PAN identifier (4-byte address field). Acknowledgment frames use a specific format. They disregard payload and addressing fields, having a total length of packet L_H=11 bytes. Equations describing one request-response event are presented below:

$$T_{event} = T_{BO}+T_{CCA}+T_{frame}(N)+T_{TA}+T_{ACK}+T_{IFS}(n)$$

$$T_{frame}(N) = 8 \cdot T_b \cdot (L_{headers} + N)$$

$$L_H = L_{PHY} + L_{MAC} + N_{address} + L_{CRC}$$

The physical layer header is 6 bytes (L_{PHY}=6), the MAC header is 3 bytes (L_{MAC}=3), and the CRC field 2 bytes long (L_{CRC}=2). Addressing fields can be as long as 20 bytes, but as it is assumed that only destination address is included, in our analysis the field is only 4 bytes long ($N_{address}$=4).

Figure 6 shows that IEEE 802.15.4 is a low data-rate standard. We analyze four physical layer variants: 868MHZ BPSK, 868MHZ ASK, 868MHz O-QPSK and 2.4GHz O-QPSK. When sending 1-byte packets, latency are 12.7 ms, 3.04 ms, 4 ms and 2.5 ms depending on the variant. When sending full 122-byte packets, latency and throughput are 61.55 ms and 2 kbps, 7.32 ms and 16.65 kbps, 14 ms and 8.64 kbps, 6.81 ms and 17.9 kbps respectively.

In the higher-throughput PHY variants, the latency is as low as 7 ms. This shows, that even if the Listen Before Talk mechanism is used according to regulatory rules, the overall

delay is negligible compared with the large delay in LoRa, which is caused by the 1% maximum duty cycle.

F. Bluetooth Low Energy (BLE)

Bluetooth Low Energy is a low-power wireless technology first defined in the Bluetooth 4.0 standard [16]. For IoT applications, it is highly preferred over Bluetooth Classic due to lower energy consumption and higher flexibility.

BLE uses the Frequency Hopping Spread Spectrum (FHSS) coding scheme, where multiple channel transmission is used to multiplex access to medium between stations. 2 M samples per second modulation (T_b=0.5 μs) is added in Bluetooth 5.0 in contrast to 1 M samples per second (T_b=1 μs) in Bluetooth 4. Bits are modulated into symbols using Gaussian Frequency Shift Keying (GFSK), with the aim to reduce interference with neighboring channels of 2.4 GHz band, since this band is widely used by other technologies, including IEEE 802.11, IEEE 802.15.4, and microwave ovens.

A BLE packet that does not include FEC starts with a 1-byte or 2-byte preamble L_{PRE} (Fig. 7). It continues with 4-byte address field L_{ADDR}. Other header fields L_{HEADS} contain 2-byte *LL* header, 4-byte *L2CAP* header and 3-byte *ATT* header resulting in 9 bytes totally. The frame is terminated by a 3-byte CRC field (L_{CRC}). Packets can be encrypted by using four optional *MIC* field bytes. Absence of MIC is assumed in the further analysis.

Optionally, BLE transmission robustness can be improved by encoding packets with FEC. Two schemes are used in the BLE Coded PHY: S=8 and S=2, where S is the number of symbols per bit, reducing the raw throughput to 125 kbps (T_{S8}=8 μs) and 500 kbps (T_{S2}=2 μs) accordingly. It uses additional fields, C1 and TERM1, which together with Preamble and Access address forms the first block of the packet (FEC1) and is encoded with the rate S=8 taking a constant T_{FEC1}=368 μs. The second block (FEC2) is encoded with rate determined by bits in C1 field – it uses the same PDU, but is terminated by CRC and TERM2 fields, which are transmitted in T_{CRC_Sx}=24×S μs and T_{TERM2_Sx}=3×S μs accordingly.

BLE Attribute Protocol (ATT) and GATT (Generic Attribute Profile) are used in the upper layers in the BLE network stack.

Preamble	Access Address	CI (Coded packet)	TERM1 (Coded packet)	Protocol Data Unit (PDU) N=2–257 bytes (uncoded) or N*8*S µs (coded)					CRC	TERM2 (Coded packet)
80 µs (coded)	256 µs (coded)	16 µs	16 µs	LL Header	Payload			MIC (optional)	3 bytes (uncoded)	3*S µs
1 byte (1M PHY)	4 byte (1M/2M PHY)			2 bytes	L2CAP Hreader	ATT Data (0-251 bytes)			24*S µs (coded)	
2 byte (2M PHY)					4 bytes	ATT Header		ATT Payload	4 bytes	
						Op Code 1 byte	Attribute Handle 2 bytes	Up to 244 bytes		

Fig. 7. BLE frame format

BLE connections last from 7.5ms to 4s. A connection is used as a communication window for each user. One communication event consists of data packet sent with the maximum of 244 bytes payload, having T_{IFS}=150 μs in between, response packet, T_{ACK}=8×T_b×L_{ACK}, as empty packet afterwards, where L_{ACK}=(Preamble + Access Address + LL Header + CRC) equals 10 or 11 bytes (in 1M and 2M mode) and IFS again. Formula for one transmission event is addressed bellow:

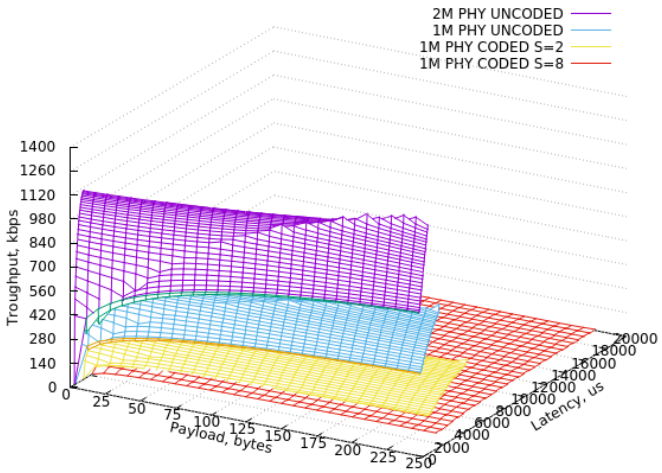

Fig. 8. BLE payload length vs. latency and throughput

$$T_{event} = T_{packet} + T_{IFS} + T_{ACK} + T_{IFS}$$

$$T_{uncoded} = 8 \cdot T_b(L_{PRE} + L_{HEADS} + N + L_{CRC})$$

$$T_{coded} = T_{FEC1} + T_{FEC2}$$

$$T_{FEC2} = 8T_{Sx}(L_{heads} + N) + T_{CRC\_Sx} + T_{TERM2\_Sx}$$

If length of an event is 1 sec, and latency for one 244 byte ATT data packet sent via 2M PHY is 1.412 ms, then we can send 1000/1.388=720 packets, which results in a maximum throughput of 1.40 Mbps.

Figure 8 shows that when sending 1 byte in 2 M and 1 M un-coded mode, latency is 416 μs and 516 μs accordingly. If full, 244 byte ATT packet is used, latency equal 1388 μs and 2460 μs, but throughput 1406 kbps and 793.5 kbps accordingly. In T_{S2} and T_{S8} coded mode, 1 byte transmission results in 1336 μs and 2236 μs latency, but if full packet is sent, latency is 5354 μs and 18254 μs, and throughput is 373 kbps and 109 kbps.

G. IEEE 802.11b

The IEEE 802.11 family of wireless standards (mostly for PHY and MAC layers) is widely used in consumer electronics and allows consumer devices to wirelessly connect to the Internet. Unlike the other technologies analyzed in this paper, IEEE 802.11 typically use TCP/IP protocols in the higher layers of the network stack. However, TCP/IP support is not a mandatory requirement for IEEE 802.11 devices, and IoT applications of IEEE 802.11 are becoming more frequent over time.

The original IEEE 802.11 standard was released in 1997, and is now considered obsolete. IEEE 802.11b [17] is one of the first amendments to original IEEE 802.11 standard. It defines three modulation techniques: DSSS, FHSS, and Diffuse Infrared. The DSSS mode offers higher bandwidth,

meaning that the other two have received comparatively little attention [31] and are not analyzed in this paper. The DSSS mode supports bandwidth of 1 Mbps (T_{1M}=1 μs) and 2 Mbps (T_{2M}=0.5 μs), when using DBPSK and DQPSK modulation respectively. Throughput can be increased to the even higher 5.5 Mbps (T_b=0.18 μs) and 11 Mbps (T_b=0.09μs) if using Complimentary Code Keying (CCK) or the optional Packet Binary Convolutional Coding.

Every IEEE 802.11b packet implements Physical Layer Convergence Protocol (PLCP), which is used to synchronize clocks, indicate physical layer parameters [17]. These services are transmitted in the PLCP Protocol Data Unit (PPDU) – with bit duration T_{1M} for a 9 byte preamble (L_{PRE}=9) and T_{2M} for 6 byte physical layer header (L_{PHY}=6). PPDU is followed by the MAC protocol data unit (MPDU), which includes control, data or management frames, and optionally uses higher bandwidth than T_{1M}/T_{2M}. Figure 9 represents a IEEE 802.11b data packet.

Preamble	PLCP Header				MAC Frame (MPDU)						
9 bytes	Signal	Service	Length	CRC	Frame Control	Duration	Addresses 1 to 3	Sequence Control	Address 4	Frame Body	FCS
	1 byte	1 byte	2 bytes	2 bytes	2 bytes	2 bytes	18 bytes	2 bytes	6 bytes	Up to 2312 bytes	4 bytes

Fig. 9. IEEE 802.11b data packet format

The IEEE 802.11b standard incorporates two medium access methods [31]: asynchronous Distributed Coordination Function (DCF) and optional synchronous Point Coordination Function. DCF is a CSMA/CA medium access algorithm, which uses Network Allocation Vector (NAV) mechanism in order to deal with packet collisions from multiple clients. It sets a packet transmission timer equal of the backoff (T_{BO}) window size. Optional Ready-To-Send (RTS) and Clear-To-Send (CTS) messages are sent to deal with the hidden terminal problem.

A transmission sequence starts with the DCF Inter-frame Spacing (DIFS) period, in which the transmitting station performs medium sensing. The period has duration of T_{DIFS}=50μs. A short IFS (SIFS) period T_{SIFS}=10 μs separates data and acknowledgment frames, which have the MAC packet length of L_{DATA}=34 bytes (Section 7.2.2 Data frames [17]) and L_{ACK}=14 bytes respectively (Section 7.2.1.3 [17]). After a successful transmission, the client goes through a mandatory backoff interval, which equals to $T_{BO}=\frac{1}{2}\times CW_{min}\times SlotTime$, where CW_{min}=31 and $SlotTime$=20 μs. This event is described in [17] sections "9.2.5.5 Control of the channel" and "9.7 Frame exchange sequences", and can contain n fragments. The latency is described by the following equations:

$$T_{event} = T_{DIFS}+T_{Data}+T_{SIFS}+T_{ACK}+T_{fragments}+T_{BO}$$

$$T_{fragments} = n \cdot (T_{Data}(N) + T_{SIFS} + T_{ACK} + T_{SIFS})$$

$$T_{Data}(N) = T_{PLCP} + 8 \cdot T_b \cdot (L_{DATA} + N)$$

$$T_{ACK} = T_{PLCP} + 8 \cdot T_b \cdot L_{ACK} + T_{SIFS}$$

$$T_{PLCP} = T_{1M} \cdot L_{PRE} + T_{2M} \cdot L_{PHY}$$

Fig. 10 shows that there is a significant improvement in throughput when the CCK coding scheme is used. Drawbacks are increased energy consumption and reduced resistance to noise compared with DSSS. Hence, DSSS is more appropriate for battery-powered sensor nodes.

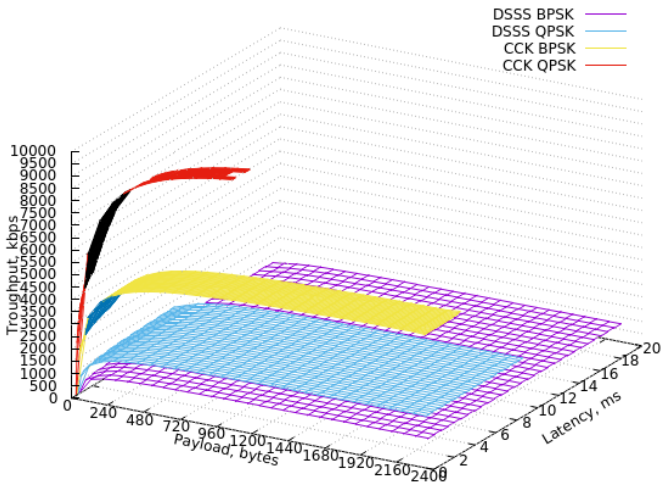

Fig. 10. IEEE 802.11b payload length vs. latency and throughput

The DSSS mode achieves 11 or 5.5 times smaller throughput compared with the case when the CCK mode is used. For example, when DSSS BPSK and DSSS DQPSK coding/modulation schemes are used to send 1-byte packets, they are finished in 818 μs and 606 μs, but when CCK is used, 471 μs and 433 μs latency is achieved.

When sending full, 2312 byte packets in the DSSS mode, 19.3 ms and 9.85 ms delay is present, while throughput is 976 kbps and 1948.7 kbps, but in the CCK mode, delay is 3.83 ms and 2.1 ms, while throughput is 5.33 Mbps and 10.56 Mbps, respectively.

H. IEEE 802.11g

The IEEE 802.11g standard [18] was ratified in 2003. It uses Extended Rate Physical OFDM (ERP-OFDM), which implements a different coding scheme, inter-frame spacing's, PPDU preamble and header compared with the ones used in IEEE 802.11b. DSSS-OFDM coding and 20 μs slot time is kept for backwards compatibility.

100 MHz ISM bandwidth is divided into thirteen overlapping 22 MHz channels, from which channels 1, 5, and 11 are non-overlapping. These three channels are often used by default. A 2 MHz reserved space in each channel is used as guard band to allow sufficient attenuation along the edge band of the channels, resulting in 20 MHz available for data transmissions.

Every channel is divided into 64 sub-carriers, each 312.5 kHz wide, using Fast Fourier transform (FFT), when encoding, and Inverse FFT (IFFT) when decoding. The center sub-carrier is not used to carry information, and 11 sub-carriers provide guard bands. This leaves four pilot sub-carriers and 48 data sub-carriers. In each 312.5 kHz (3.2 μs) sub-carrier, a

0.8 μs long period is used as the guard band, leaving 2.4 μs as the usable bit period. This translates to 250 kbaud symbol rate per sub-carrier, and 12 Mbaud symbol rate per whole channel.

PLCP Preamble		Signal					Data					
10 Short OFDM Symbols	2 Long OFDM Symbols	Rate	Reserved	Length	Parity	Tail	Service	MPDU			Tail	Pad Bits
								Header	Frame Body	FCS		
		4 bits	1 bit	12 bits	1 bit	6 bits	16 bits	30 bytes	Up to 2312 bytes	4 bytes	6 bits	Up to 1 Symbol

Fig. 11. IEEE 802.11g data packet format

In an IEEE 802.11g frame (Fig. 9) preamble is transmitted as ten short (12 sub-carriers) and two long symbols (48 sub-carriers), with the total length of 16 μs, but PLCP (signal field), with 6 Mbps BPSK 1/2 rate coding and total length of 4 μs, resulting in header length of T_{PLCP_H}=20 μs [32].

IEEE 802.11g varies modulation and coding schemes (MCS) depending on the quality of the link. The MCS is stored in a 4-bit *Rate* field. Depending on the modulation (BPSK, QPSK, 16 QAM or 64 QAM), coded bits per sub-carrier vary accordingly: N_{BPSC}={1, 2, 4, 6} and coded bits per OFDM symbol (all 48 sub-carriers) N_{CBPS}={48, 96, 192, 288}, which results in the throughput of f_{data}={12 Mbps, 24 Mbps, 48 Mbps and 72 Mbps} accordingly. Furthermore, all four modulation types are enhanced by Convolution Coding with one of the fallowing coding rates *CR*={1/2, 2/3, 3/4}, resulting in 16 MCS indexes (hence the 4-bit *Rate* field), which have the raw bit length of T_b=(1/f_{data})×*CR*.

The PLCP *Data* field contains the same 34 byte MPDU as in IEEE 802.11b (14 bytes in case of an ACK). This is succeeded by a 2-byte *Service* field and 6 bit tail resulting in L_{DATA} = 294 bits and L_{ACK} = 102 bits. Some padding bits are added so that number of bits in PLCP Data field is a multiple of the N_{CBPS} bits, since the data is not transmitted in standalone bits, but in whole symbols. Least common multiple (LCM) is assessed in the equations below, where $\lceil\{a,b\}\rceil$ is equal to $\lceil a/b\rceil \times b$, as used in [32]; however, our calculations do not assume variable payload length.

Backoff period T_{BO} estimation, as well as DCF medium access algorithm are the same as in the IEEE 802.11b standard. The slot time is reduced to 9 μs, and other variables to T_{DIFS}=28 μs, T_{SIFS}=10 μs and CW_{min}=15.

$$T_{event} = T_{DIFS} + T_{Data}(N) + T_{SIFS} + T_{ACK} + T_{fragments} + T_{BO}$$

$$T_{fragments}(n) = n \cdot (T_{Data}(N) + T_{SIFS} + T_{ACK} + T_{SIFS})$$

$$T_{Data}(N) = T_{PLCP\_H} + T_b \cdot \lceil\{L_{DATA} + 8 \cdot N, N_{CBPS}\}\rceil$$

$$T_{ACK} = T_{PLCP\_H} + T_b \cdot \lceil\{L_{ACK}, N_{CBPS}\}\rceil$$

The graph in Fig. 12 shows the performance visualization based on these equations. The same equations apply to the IEEE 802.11a standard for the US market, since the available bandwidth and OFDM mechanism is the same.

When sending 1-byte data packets, the latency in BPSK, QPSK, 16-QAM and 64QAM coding schemes is 0.2 ms, 0.18 ms, 0.16 ms, and 0.16 ms. On the other hand, when transmitting full 2313-byte packets, the latency is 2.25 ms, 1.2 ms, 0.67 ms, and 0.5 ms, but throughput is 8.5 Mbps, 16.5 Mbps, 31.45 Mbps, and 44.31 Mbps, respectively.

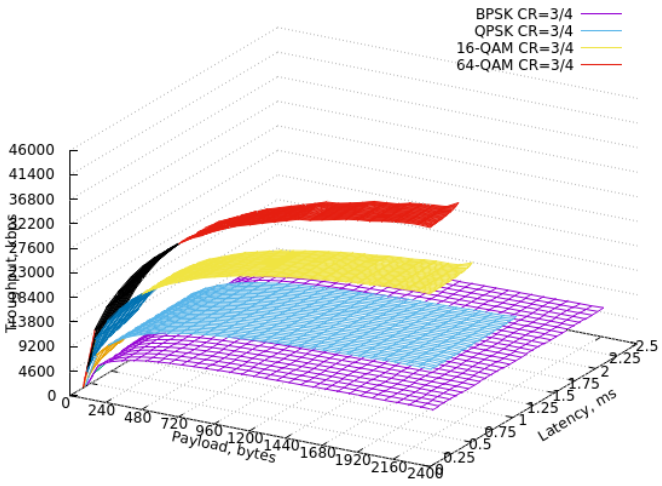

Fig. 12. IEEE 802.11g payload length vs. latency and throughput

I. IEEE 802.11n

The IEEE 802.11n standard amendment [19] was published in 2009. It brings several new extensions to IEEE 802.11g PHY and MAC layer mechanisms, with the main aim to achieve a higher throughput. These extensions include dual band (2.4 GHz/5 GHz) and dual bandwidth (20/40 MHz) modes, increased number of data sub-carriers to 52 (108 in 40 MHz channel mode) and optional short guard intervals (GI) of 4 μs, resulting in increased total symbol bandwidth of 13 MHz (long GI) and 14.4 MHz (short GI) if 20 MHz channel size is used, and symbol bandwidth of 27 MHz and 30 MHz for 40 MHz channels.

The IEEE 802.11n MAC layer includes a modified channel access method. Packets are prioritized prior to transmission by Enhanced Distributed Coordination Access (EDCA), firstly introduced in IEEE 802.11e. Furthermore, the MAC layer is enhanced by frame aggregation, so that two or more data frames can be sent in a single transmission, using MAC service data unit (A-MSDU) aggregation and MAC protocol data unit (A-MPDU) aggregation. Moreover, block acknowledgment (BACK), allows communication of series of multiple data frames, which are then jointly acknowledged by single BACK frame.

If aggregation is not used, PPDU and MPDU fields resemble the ones in IEEE 802.11g (QoS and High Throughput Control 2-byte fields are still included). A typical IEEE 802.11n packet is shown in Fig. 13 and includes frame aggregation in order to better demonstrate the differences in comparison with the previous IEEE 802.11 standards. OFDM training fields (PLCP header) takes 24 μs to transmit, in addition to a number of data and extension HT-LTFs fields, each of which takes 4 μs.

The IEEE 802.11n standard also introduces MIMO (Multiple-Input and Multiple-Output) support. However, the case of IoT systems, a simple 1x1 MIMO (1 antenna) is typically used due to low power requirements. In this case, the data and extension HT-LTFs together take 8 μs, resulting

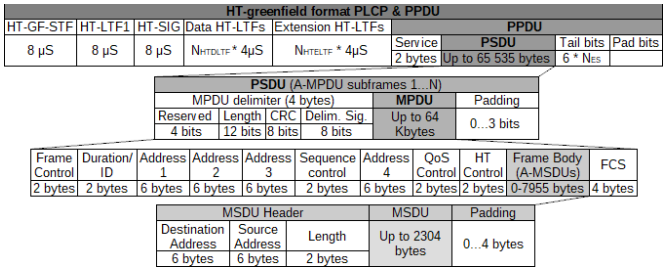

Fig. 13. IEEE 802.11n data packets using frame aggregation

in T_{PLCP_H}=32 μs.

The implementation of the aggregation mechanism is extremely memory intensive and hence very difficult to implement on the client, even more so if the client is an embedded IoT system. Therefore we further consider an implementation that supports only a single MSDU and MPDU packet, similar to IEEE 802.11b/g. Only the *Frame control*, *Duration/ID*, *Address 1*, *Sequence control* and *FCS* fields are mandatory. Depending on the packet type (control, management or data) they are combined with other optional fields [19].

Modulation and coding (MCS) scheme is identical to one used in IEEE 802.11g, therefore N_{BPSC} is also equivalent. Since the number of data sub-carriers is increased (52 in the 20 MHz mode), N_{CBPS}={52, 104, 208, 312}, which results in long GI throughput f_{data}={13 Mbps, 26 Mbps, 52 Mbps and 78 Mbps} and short GI throughput f_{data}={14.4 Mbps, 28.9 Mbps, 57.8 Mbps and 86.7 Mbps} accordingly.

Furthermore, all four modulation types are enhanced by Convolution Coding with one of the following coding rates CR={1/2, 3/4, 2/3, 5/6}, resulting in 127 MCS indexes (hence the 7-bit *Rate* field of HT SIGNAL field), which also depends on spatial streams, modulation type, guard interval length and 20/40MHz bandwidth mode, and have the raw bit length of: $T_b=(1/f_{data})\times CR$.

The PLCP *Data* field contains the variable length Frame Body and a constant, L_{DATA}=320 bit (40 byte) MPDU, which is 6 bytes longer than the IEEE 802.11b/g MPDU, since it uses 2-byte *QoS control* and 4-byte *HT control* fields. The management frame does not include 6-byte *Address4* and 2-byte *QoS* fields, and is used for configuring the network, e.g., setting frame aggregation and block ACK mechanism by an exchange of 34 byte BACK action (ADDBA) management Request/Response frames. Control frames are sent encapsulated into control wrapper frames, which use the mandatory fields plus HT control field and are of constant length (L_{ACK}=168 bits or 22 bytes). Padding bits are added in same manner as in IEEE 802.11g.

Four different priority queues (voice, video, best effort and background) are defined to allow to implement QoS. Channel access with different values of Arbitrated Inter-Frame Spacing (AIFS) is used, and replaces the single DCF legacy DIFS interval. T_{SIFS} and slot time match IEEE 802.11g values: 10 μs and 9 μs, respectively. The AIFS period equals to T_{SIFS}

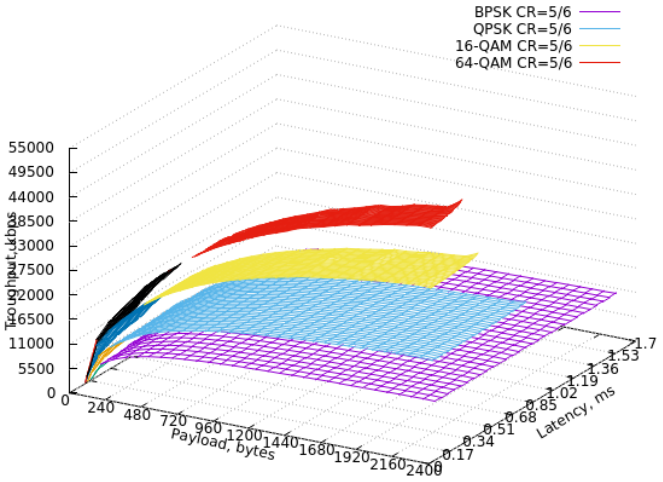

Fig. 14. IEEE 802.11n payload length vs. latency and throughput

value plus a variable number of slot times (AIFSN), which depend on access category. Assuming the voice queue is used, AIFSN[AC]=2 and AIFS=10 μs+2×9 μs=28 μs.

Each of the four priority queues has a defined Contention Window range, which affect the backoff period. The backoff period is calculated in the same way as in IEEE 802.11g: $T_{BO}=\frac{1}{2}\times CW_{min}\times$SlotTime. For voice channel CW_{min}=3, which makes T_{BO}=13.528 μs.

The equation below is the same as the corresponding equation for IEEE 802.11g, except thatT_{DIFS} interval is replaced with T_{AIFS} interval:

$$T_{event} = T_{AIFS}+T_{Data}+T_{SIFS}+T_{ACK}+T_{fragments}+T_{BO}$$

Figure 14 shows that IEEE 802.11n can achieve very low latency compared with the other surveyed technologies. When sending 1-byte packets, with different modulation, but the same coding rate (5/6) the latency is 160 μs, 141 μs, 128 μs, and 128 μs. When sending 2312 byte packets the latency is 1700 μs, 900 μs, 510 μs, and 384 μs, but throughput is the theoretical maximum: 11 Mbps, 21 Mbps, 38 Mbps and 52 Mbps.

III. Discussion

This section summarizes and compares the surveyed technologies. A numerical comparison is given in Figs. 15–17, which show the throughput, latency and packet overhead metrics for all surveyed technologies.

A. Technologies

NFC is very different from the other technologies analyzed in this paper, largely due to the fact that it utilizes different physical principles for communication. In NFC radio waves are transmitted in the near field (i.e. in the region of the electromagnetic field close to the antenna); the other technologies analyzed in this paper use the far field. In NFC in the maximum range of 5 cm, where other standards can achieve a range of 100 m or more. The maximum frame length in NFC

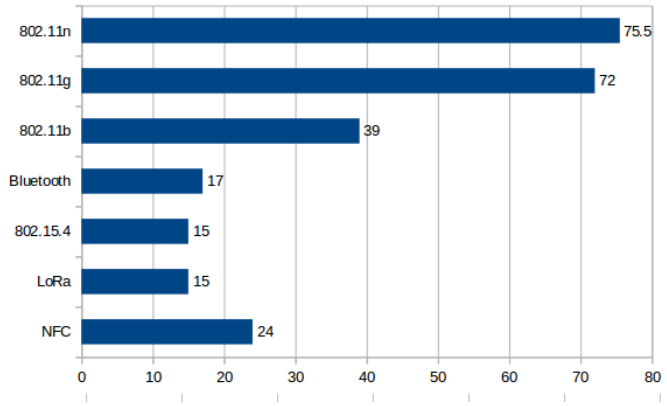

Fig. 15. Packet overhead comparison

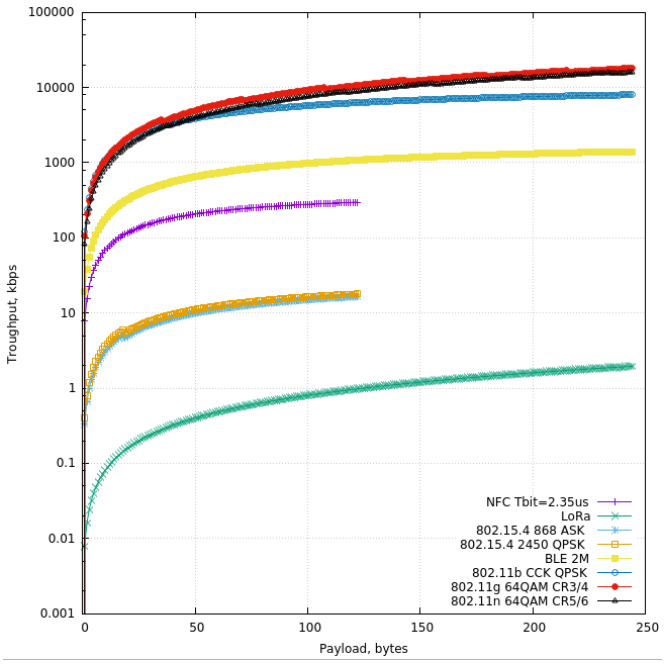

Fig. 16. Throughput vs. payload

is 122 bytes; with frames this long, the maximum throughput of 255 kbps can be achieved.

LoRa uses a chirp spread spectrum modulation scheme, which allows it to achieve the highest receiver sensitivity among the other standards, resulting in impressive a link budget and communication range of up to 10 km, as well as very low power consumption. LoRa makes a tradeoff between the throughput and receiver sensitivity. Sensitivity on the order of −130 dBm is achieved, but leads to a very low data rate of 1952 bps, assuming that the mandatory duty cycle restrictions for transmissions are followed. However, LoRa is advantageous in many cases, as its main application is in low-rate sensor networks where each device sends sensor data only a couple times per day. The packet overhead is 13 to 15 bytes for downlink/uplink packets, plus 10.25 preamble symbols.

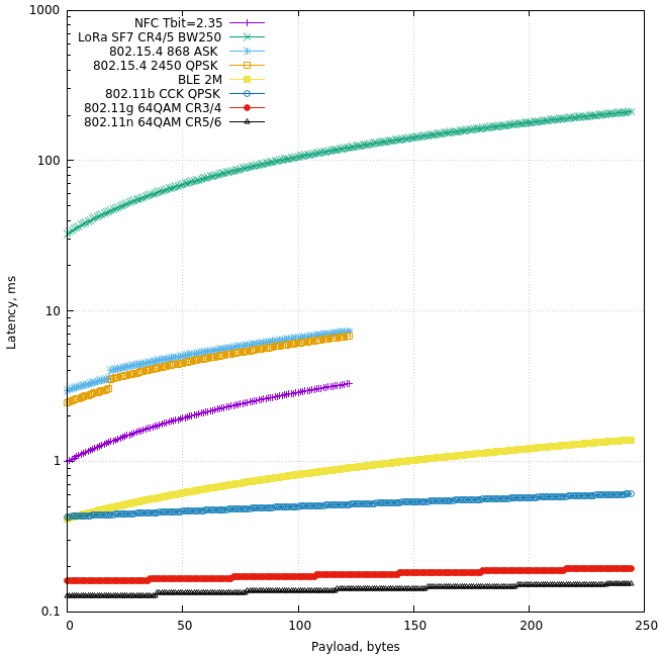

Fig. 17. Latency vs. payload

IEEE 802.15.4 is a lightweight protocol which by default header overhead of only 15 bytes. In its higher throughput modulation schemes, latency is 7 ms at most. This shows that even if the listen-before-talk mechanism is implemented according to regulatory rules, the latency is negligible compared with the latency of LoRa. Fig. 17 shows that latency suddenly increases at 19 byte payload region, because IFS period increases by 448 μs. Because of the simplicity of its physical layer, IEEE 802.15.4 does not require an extensive processing power from the transceiver devices. Furthermore, the DSSS coding scheme allows it to be more robust against narrow-band interference than BLE.

BLE allows a higher PHY layer throughput than the standards described above: up to 2 Mbps, resulting in a lower achievable latency. Unlike IEEE 802.15.4, BLE also includes adaptive frequency hopping. BLE 5.0 also adds support for different coding rates. Finally, BLE is a very widely used technology: every smartphone and many computers include BLE transceivers. This allows IoT devices to seamlessly connect with existing infrastructure using BLE, giving it a huge advantage compared with LoRa and IEEE 802.15.4 for many applications, such as wearable electronics. Finally, the connection mode of BLE allows efficient point-to-point information transmission, while the advertisement mode allows to broadcast and support energy-efficient collection and dissemination of low-rate and periodic data.

The IEEE 802.11 family of standards has a different application focus than the other technologies surveyed in this article. IEEE 802.11 protocols are primarily optimized for throughput. As a result, IEEE 802.11 allows much larger packets (>1500 bytes) and higher bitrates than the other

technologies, resulting in higher energy-efficiency per a bit in case a large stream of data has to be transmitted between two nodes. However, assuming a more typical IoT application that uses short and infrequent packets, per-packet overhead is larger in IEEE 802.11, and energy requirements higher. Furthermore, connection establishment is required to communicate, further adding to the energy requirements.

IEEE 802.11b is an old standard, but most WiFi devices are still compatible with it. It uses the DSSS coding scheme, which allows it to perform reliable transmissions and makes it suitable for industrial use cases. IEEE 802.11b/g/n standards are implemented in many popular embedded systems-on-chip such as ESP8266.

IEEE 802.11g/n standards use OFDM physical layer, which increases throughput five times or even more compared with IEEE 802.11b. The IEEE 802.11n standard implements a QoS mechanism to reduce latency and prioritized traffic. Fig. 15 shows that IEEE 802.11g/n standard packets have headers of 70+ bytes, therefore these standards are not optimized for sending short packets. In IEEE 802.11n, frame aggregation and MIMO are introduced as well, with the aim to achieve higher throughput. However, if these features are used, they drastically increase computational requirements and energy consumption, therefore are not suitable for low-power IoT systems.

B. Overall Trends

Overall, this analysis show the following trends in the evolution of low-power wireless technologies:

- *Increased complexity.* New standards start up simple (e.g., IEEE 802.11b, IEEE 802.15.4-2006). With time, they become more complex as a plethora of new features are added (e.g., IEEE 802.11g/n, IEEE 802.15.4-2015).
- *Convergence.* Many standards share the same broad application area, for example, data collection from low-rate sensors. It is therefore not a surprise that successful features are added as the standards evolve: for example, channel hopping has been added to IEEE 802.15.4-2015 after it was present in Bluetooth for more than a decade; on the other hand, support for low-power multi-hop networks has been adopted in the opposite direction, with Bluetooth Mesh being standardized only in 2017. Similarly, features initially present in IEEE 802.11 have been adopted: OFDM was added to IEEE 802.15.4-2016 (although only for the sub-GHz bands); support for run-time switching of PHY-layer data rates was added both to IEEE 802.15.4-2016 and BLE 5.0.
- *Specialization.* The direction of this trend is opposite to that of convergence. In this case, new features make the standards more targeted towards specific applications. This form of evolution is mostly seen in the IEEE 802.11 family of standards. For example, the IEEE 802.11n standard sacrifices energy consumption for throughput, and is therefore less suitable for low-power IoT networks than the IEEE 802.11b standard.

IV. Related Work

Most surveys on the low-power wireless limit their scope to a single technology, or to a single application domain. For instance, Gomez *et al.* [33] overview Bluetooth Low Energy. They explore its potential applications and investigate the impact of various parameters on its performance. Friesen *et al.* [2] survey the use of Bluetooth in intelligent transportation systems. Yin *et al.* [34] survey the Bluetooth 5.0 and Bluetooth Mesh standards.

Bhoyar *et al.* [35] present a comparative survey of IEEE 802.11a/b/g/n standards. Tsao *et al.* [36] survey MAC protocols for energy-efficient operation of IEEE 802.11 networks. Siekkinen *et al.* [37] compare the energy consumption of BLE and IEEE 802.15.4/ZigBee. They conclude that BLE is indeed more energy efficient due to its more efficient spectrum use (no DSSS) and higher transmission rate.

De Guglielmo *et al.* [38] survey the IEEE 802.15.4e amendment of the IEEE 802.15.4 standard (later incorporated in IEEE 802.15.4-2015). This amendment introduces multiple new MAC modes to the standard, including the Time Slotted Channel Hopping (TSCH) MAC mode. They identify weaknesses in the previous version of the standard and discuss how the new amendment addresses them.

In a recent work, Sundaram *et al.* [39] overview the LoRa protocol and identify research problems and open issues connected to it. Margelis *et al.* [40] overview LoRa for industrial applications.

NFC is surveyed by many papers, for example by Coskun *et al.* [41]. They present its communication essentials along with other aspects, including the ecosystem and applications.

Xu *et al.* [42] survey the usage of IoT technologies in industries; however, they only present a broad overview and do not study which wireless technologies are suitable for industrial applications.

In the context of this related work, our main contribution is a comparative study of multiple technologies, along with a quantitative comparison between multiple performance metrics of these technologies.

V. Conclusions

This paper investigates a number of popular wireless technologies, with a particular focus on low-power wireless technologies for IoT applications. Based on timing and packet format information from the standards of these technologies, we investigate the relation between packet size, latency and throughput. We show that trade-offs in multiple dimensions can be made, and that unsurprisingly there is no single "best" low-power wireless technology. We hope that this paper will be useful to IoT practitioners interested in choosing a wireless technology for their next IoT project.

References

[1] A. Naimat, "The internet of things market: A data-driven analysis of companies developing and adopting iot technology," Apr. 2014.

[2] M. R. Friesen and R. D. McLeod, "Bluetooth in intelligent transportation systems: a survey," *International Journal of Intelligent Transportation Systems Research*, vol. 13, no. 3, pp. 143–153, 2015.

[3] N. Barkovskis, A. Salmins, K. Ozols, M. A. M. García, and F. P. Ayuso, "WSN based on accelerometer, GPS and RSSI measurements for train integrity monitoring," in *2017 4th International Conference on Control, Decision and Information Technologies (CoDIT)*, pp. 0662–0667, IEEE, 2017.

[4] A. Elsts, X. Fafoutis, G. Oikonomou, R. Piechocki, and I. Craddock, "TSCH Networks for Health IoT: Design, Evaluation, and Trials in the Wild," *ACM Transactions on Internet of Things*, vol. 1, no. 2, pp. 1–27, 2020.

[5] I. Yaqoob, I. A. T. Hashem, Y. Mehmood, A. Gani, S. Mokhtar, and S. Guizani, "Enabling communication technologies for smart cities," *IEEE Communications Magazine*, vol. 55, no. 1, pp. 112–120, 2017.

[6] D.-M. Han and J.-H. Lim, "Smart home energy management system using IEEE 802.15.4 and ZigBee," *IEEE Transactions on Consumer Electronics*, vol. 56, no. 3, pp. 1403–1410, 2010.

[7] M. Rizzi, P. Ferrari, A. Flammini, E. Sisinni, and M. Gidlund, "Using LoRa for industrial wireless networks," in *2017 IEEE 13th international workshop on factory communication systems (WFCS)*, pp. 1–4, IEEE, 2017.

[8] M. Čech, A.-J. Beltman, and K. Ozols, "I-MECH–Smart System Integration for Mechatronic Applications," in *2019 24th IEEE International Conference on Emerging Technologies and Factory Automation (ETFA)*, pp. 843–850, IEEE, 2019.

[9] Nordic Semiconductors, *nRF52840 Product Specification v1.1*, 02 2019. https://infocenter.nordicsemi.com/pdf/nRF52840_PS_v1.1.pdf.

[10] ITU, "Radio regulations," *Chapter II – Frequencies, Section IV–Table of Frequency Allocations*, 2016.

[11] A. Kivimäki, R. Naturalium, and R. Ahonen, "Wireless telecommunication standardization processes—actors' viewpoint," 2007.

[12] A. Harney and C. O'Mahony, "Wireless short-range devices: Designing a global license-free system for frequencies¡ 1 ghz," *Analog Dialogue*, vol. 40, no. 1, pp. 18–22, 2006.

[13] V. Coskun, B. Ozdenizci, and K. Ok, "A survey on near field communication (NFC) technology," *Wireless personal communications*, vol. 71, no. 3, pp. 2259–2294, 2013.

[14] A. Augustin, J. Yi, T. Clausen, and W. M. Townsley, "A study of LoRa: Long range & low power networks for the Internet of Things," *Sensors*, vol. 16, no. 9, p. 1466, 2016.

[15] "Part 15.4: wireless medium access control (MAC) and physical layer (PHY) specifications for low-rate wireless personal area networks (LR-WPANs)," *IEEE Computer Society*, 2011. LAN/MAN Standards Committee and others.

[16] Bluetooth SIG., *Bluetooth Core Specification 5.0.*, 12 2016. Vol. 6. - Low Energy Controller.

[17] IEEE 802.11 Working group *et al.*, "Part 11: wireless LAN medium access control (MAC) and physical layer (PHY) specifications: higher-speed physical layer extension in the 2.4 GHz band," *ANSI/IEEE Std 802.11*, 1999.

[18] IEEE 802.11 Working group, "IEEE Std. 802.11g. Supplement to Part 11: Wireless LAN Medium Access Control (MAC) and Physical Layer (PHY) Specifications: Higher-speed Physical Layer Extensions in the 2.4 GHz Band," *IEEE Std. 802.11g-2003*.

[19] IS Association *et al.*, "802.11-2012-IEEE Standard for Information technology-Telecommunications and information exchange between systems Local and metropolitan area networks-Specific requirements Part 11: Wireless LAN Medium Access Control (MAC) and Physical Layer (PHY) Specifications," *Retrived from*, 2012.

[20] S. Olivieri, "An investigation of security in near field communication systems," 2015.

[21] "Standard ECMA–340: Near Field Communication Interface and Protocol (NFCIP-1)," 2013. Ecma International.

[22] M. Bor and U. Roedig, "LoRa transmission parameter selection," in *2017 13th International Conference on Distributed Computing in Sensor Systems (DCOSS)*, pp. 27–34, IEEE, 2017.

[23] M. J. Abbas, M. Awais, and A. U. Haq, "Comparative analysis of wideband communication techniques: Chirp spread spectrum and direct sequence spread spectrum," in *2018 International Conference on Computing, Mathematics and Engineering Technologies (iCoMET)*, pp. 1–6, IEEE, 2018.

[24] N. Sornin, M. Luis, T. Eirich, T. Kramp, and O. Hersent, "LoRaWAN Specification 1.0," *LoRa Alliance*, 2015.

[25] D. Bankov, E. Khorov, and A. Lyakhov, "On the limits of LoRaWAN channel access," in *2016 International Conference on Engineering and Telecommunication (EnT)*, pp. 10–14, IEEE, 2016.

[26] P. Ferrari, A. Flammini, M. Rizzi, E. Sisinni, and M. Gidlund, "On the evaluation of LoRaWAN virtual channels orthogonality for dense distributed systems," in *2017 IEEE International Workshop on Measurement and Networking (M&N)*, pp. 1–6, IEEE, 2017.

[27] M. Loy, R. Karingattil, and L. Williams, "ISM-band and short range device regulatory compliance overview," *Texas Instruments*, 2005.

[28] "IEEE Standard for Local and metropolitan area networks—Part 15.4." IEEE Std 802.15.4-2015, 2015.

[29] W. Kastner, C. Reinisch, and K. Lukas, "IEEE 802.15.4 MAC API," 5 2008.

[30] B. Latré, P. De Mil, I. Moerman, N. Van Dierdonck, B. Dhoedt, and P. Demeester, "Maximum throughput and minimum delay in ieee 802.15.4," in *International Conference on Mobile Ad-Hoc and Sensor Networks*, pp. 866–876, Springer, 2005.

[31] B. E. Henty, "A Brief Tutorial on the PHY and MAC layers of the IEEE 802.11b Standard," *White paper, Intersil*, 2001.

[32] M.-J. Ho, J. Wang, K. Shelby, and H. Haisch, "IEEE 802.11 g OFDM WLAN throughput performance," in *2003 IEEE 58th Vehicular Technology Conference. VTC 2003-Fall (IEEE Cat. No. 03CH37484)*, vol. 4, pp. 2252–2256, IEEE, 2003.

[33] C. Gomez, J. Oller, and J. Paradells, "Overview and evaluation of Bluetooth Low Energy: An emerging low-power wireless technology," *Sensors*, vol. 12, no. 9, pp. 11734–11753, 2012.

[34] J. Yin, Z. Yang, H. Cao, T. Liu, Z. Zhou, and C. Wu, "A survey on Bluetooth 5.0 and mesh: New milestones of IoT," *ACM Transactions on Sensor Networks (TOSN)*, vol. 15, no. 3, pp. 1–29, 2019.

[35] Bhoyar, Rahul and Ghonge, Mangesh and Gupta, Suraj, "Comparative Study on IEEE Standard of Wireless LAN/Wi-Fi 802.11 a/b/g/n," *International Journal of Advanced Research in Electronics and Communication Engineering (IJARECE)*, vol. 2, no. 7, pp. 687–691, 2013.

[36] S.-L. Tsao and C.-H. Huang, "A survey of energy efficient MAC protocols for IEEE 802.11 WLAN," *Computer Communications*, vol. 34, no. 1, pp. 54–67, 2011.

[37] M. Siekkinen, M. Hiienkari, J. K. Nurminen, and J. Nieminen, "How low energy is Bluetooth Low Energy? Comparative measurements with ZigBee/802.15.4," in *2012 IEEE wireless communications and networking conference workshops (WCNCW)*, pp. 232–237, IEEE, 2012.

[38] D. De Guglielmo, S. Brienza, and G. Anastasi, "IEEE 802.15.4e: A survey," *Computer Communications*, vol. 88, pp. 1–24, 2016.

[39] J. P. S. Sundaram, W. Du, and Z. Zhao, "A survey on LoRa networking: Research problems, current solutions, and open issues," *IEEE Communications Surveys & Tutorials*, vol. 22, no. 1, pp. 371–388, 2019.

[40] G. Margelis, R. Piechocki, D. Kaleshi, and P. Thomas, "Low throughput networks for the IoT: Lessons learned from industrial implementations," in *2015 IEEE 2nd world forum on internet of things (WF-IoT)*, pp. 181–186, IEEE, 2015.

[41] V. Coskun, B. Ozdenizci, and K. Ok, "A survey on near field communication (NFC) technology," *Wireless personal communications*, vol. 71, no. 3, pp. 2259–2294, 2013.

[42] L. Da Xu, W. He, and S. Li, "Internet of Things in Industries: A Survey," *IEEE Transactions on industrial informatics*, vol. 10, no. 4, pp. 2233–2243, 2014.